Chapter 2: THE ONE-PLUS-ONE RUNUP MODEL

This chapter presents a variable grid finite-differences approximation of the characteristic form of the shallow-water-wave equations without artificial viscosity or friction factors to model the propagation and runup of one-dimensional long waves. This model is referred to as VTCS-2 and is applied to the calculation of the evolution of breaking and nonbreaking waves on sloping beaches. Then, the computational results are compared with the analytical solutions, other numerical computations and with laboratory data for breaking and nonbreaking solitary waves. The model is found to describe the evolution and runup of nonbreaking waves very well, even when using a very small number of grid points per wavelength. Even though the method does not model the detailed surface profile of wave breaking well, it adequately predicts the runup of plunging solitary waves without ad-hoc assumptions about viscosity and friction. This appears to be a further manifestation of the well-documented but unexplained ability of the shallow water wave equations to provide quantitatively correct runup results even in parameter ranges where the underlying assumptions of the governing equations are violated.

2.1 Introduction

The problem of determining the two-dimensional evolution (propagation over one-dimensional topography) and runup of long waves on a sloping beach is a classic problem in hydrodynamics. Analytical solutions for the runup of nonbreaking sinusoidal, cnoidal and sol-

itary waves exist, and recently there have been reports of numerical solutions for breaking periodic, solitary and N-waves. The understanding of the solution of this 1+1 problem is believed to be of importance for solving the 2+1 runup problem, i.e., two propagation dimensionless (Liu et al. 1991). To this end, the National Science Foundation of the United States has funded a multicenter study to document existing 2-D and 3-D codes now under development and the results were compared in the 1995 International Workshop of Long Wave Runup, in Friday Harbor, Washington.

There is one analytical (Synolakis 1987a, Tadepalli and Synolakis 1994) and four existing numerical formulations to the canonical problem 2-D long wave problem, i.e., a long wave propagating over constant depth first and then climbing up a sloping beach. Three formulations are essentially 1-D depth-averaged approximations of the 2-D problem, i.e., solutions of the shallow water wave equations using the method of characteristics, using Lax-Wendroff-type conservation scheme and solutions of the Boussinesq equations. Solutions of the 2-D "potential" flow problem are now available. These approaches will be described below. Our method is a novel variable-grid finite difference solution of the shallow water wave equations, with certain distinct advantages to both solutions based on the method of characteristics or on the Lax-Wendroff scheme.

Stoker (1957) presented perhaps the first numerical solution of the shallow-water wave equations using the method of characteristics for a sloping beach. The advantage of this method is the exact relationship between physical variables along the characteristic lines for simple bottom topography. The path of the shoreline during runup or rundown is

a characteristic line allowing for efficient and direct computation of the shoreline path. The method produced very accurate results for simple cases, but a new computational space grid had to be calculated every time step. When characteristic lines crossed at the breaking point, the shoreline evolution had to be treated in a different manner. Since Stoker's work, more evolved solution methods (Freeman and Le Mehaute 1964, Iwasaki and Togashi 1970) improved the computational efficiency, but they predicted runup values which differed substantially from laboratory observations. Also for non-uniformly sloping beaches, this method is cumbersome. The method of characteristics has now been largely abandoned.

Finite-difference type methods use time-independent space grids; unknown variables are computed at fixed grid points distributed over the computational area. To allow for the possible calculation of bore propagation, Hibbert and Peregrine (1979) proposed solving the equations in their conservation form using the Lax-Wendroff scheme (Richtmeyer and Morton 1968); they were able to calculate the evolution of a uniform bore up a sloping beach. Their work was ground-breaking; before then it had not been possible to calculate wave runup and obtain physically realistic solutions. The problem had been the numerical treatment of the moving boundary past the initial shoreline. Although their initial algorithm was not very robust (see discussion in Synolakis 1986, 1989), subsequent versions (Packwood and Peregrine 1981, Kobayashi et al. 1987) further refined this practice to what is now the most popular method for solving the shallow water wave equations. However, the critical and supercritical flow conditions in the vicinity of the shoreline, i.e., when the Froude number is greater than one, often causes numerical instabilities (Synolakis

1989). To suppress them, Packwood (1980) and Kobayashi and associates (1987, 1989, 1990, 1994) used additional dissipative terms in the finite-difference equations. Rumming and Kowalik (1980) and Kowalik and Bang (1987) used a stabilizing algorithm at regular intervals of time or filtering of the numerical solution. All these methods introduce ad-hoc additional parameters such as artificial viscosity coefficients and friction factors. Even though many of these solutions work well for practical problems, the need to identify adequate values for these additional parameters diminishes their appeal.

Nonbreaking numerical solutions of the Boussinesq equations for the canonical problem are reviewed by Liu et al (1991). Briefly, Goto (1979) proposed a Lagrangian formulation of the Boussinesq equations and Goto and Shuto (1983) solved these equations by introducing an artificial viscosity term. Zelt (1991) developed a Lagrangian finite-element method for calculating the runup of breaking solitary waves; his solution uses an artificial viscosity term and a friction term. With the exception of the profile of waves at breaking, his method produces superior modeling of nonbreaking-wave laboratory experiments, if only one calibrates the model with laboratory maximum runup data known a priori.

Nonbreaking BEM solutions of the two-dimensional potential flow approximation of the canonical problem were introduced by Dold and Peregrine (1986). These methods solve Laplace's equation directly subject to the unadulterated forms of the kinematic and dynamic boundary conditions, and they allow for calculating of the vertical structure of the velocity field. Grilli et al. 1989, Subramanya and Grilli (1994) and Grilli et al. (1994) pro-

posed a very robust solution for the calculation of the runup of solitary waves with initial height close to the limiting wave height. This by itself was a remarkable achievement, not only because they demonstrated good agreement with laboratory data, but also because, apparently, their method does not include any ad-hoc coefficients and it does not need to be calibrated. However, even though they have considered breaking waves, they have calculated their evolution up to the breaking point, but not the maximum runup. Also, this method is still quite computationally intensive limiting the size of the flow domain which can be modeled.

Here, a new variable-grid finite-difference formulation of the shallow water wave equations is presented which allows the calculation of the evolution of breaking waves without introducing any ad-hoc coefficients. The method is simple, explicit and direct, and it produces excellent agreement with laboratory data for the maximum runup of nonbreaking and breaking waves. The method also predicts wave evolution profiles which adequately model the laboratory observations. The computational simplicity and efficiency of this method makes it suitable for calculations over two-dimensional topography. This model will be henceforth referred to as VTCS-2.

2.2 Mathematical formulation

Consider the propagation of long waves in a one-dimensional channel with variable depth as in Figure 2.1. The physical problem is described by the shallow-water-wave equations:

$$\begin{aligned} h_t + (uh)_x &= 0 \\ u_t + uu_x + gh_x &= gd_x, \end{aligned} \tag{2.1}$$

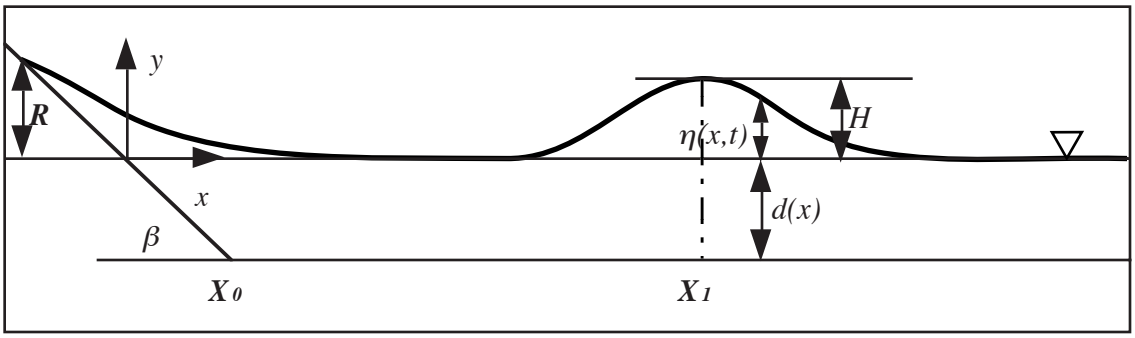

Figure 2.1 Definition sketch for solitary wave climbing up sloping beach

with the initial conditions

$$\begin{aligned} h(x,0) &= h_0(x), \\ u(x,0) &= u_0(x), \end{aligned} \tag{2.2}$$

where $h(x,t) = \eta(x,t) + d(x)$, $\eta(x,t)$ is the wave amplitude, $d(x)$ is the undisturbed water depth, $u(x,t)$ is the depth-averaged velocity, g is the acceleration of gravity. The origin of the coordinate system is at $x = 0$, and x increases monotonically seaward.

To solve boundary value problems for (2.1) the shallow-water equations are written in characteristic form. The system of equations (2.1) is a hyperbolic system with all real and different eigenvalues and it can be written in a characteristic form as follows,

$$\begin{aligned} p_t + \lambda_1 p_x &= g d_x \\ q_t + \lambda_2 q_x &= g d_x \ , \end{aligned} \tag{2.3}$$

where $p = u + 2\sqrt{gh}$, $q = u - 2\sqrt{gh}$ are the "Riemann invariants" (for short) of this system and $\lambda_{1,2} = u \pm \sqrt{gh}$ are the eigenvalues.

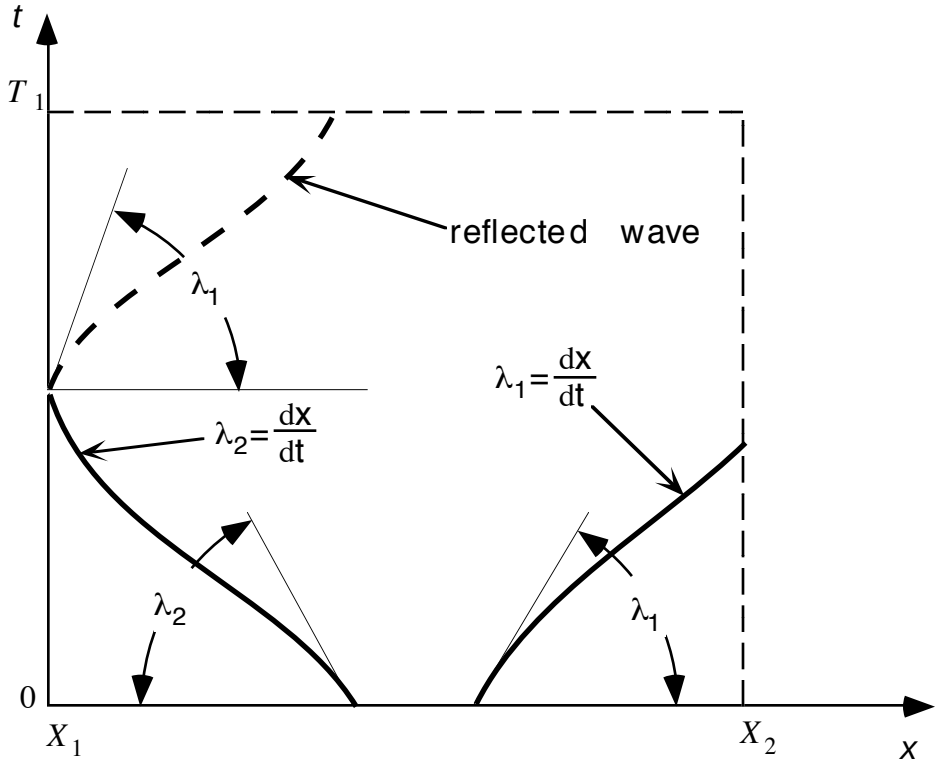

Figure 2.2 Sketch of the characteristic lines of the equations (2.3).

The characteristic form of the equations is used to establish well-posed boundary conditions for fixed boundaries. Consider solution of the equations (2.3) in the area with fixed boundaries $x = X_1$ and $x = X_2$ in space and within time interval from $t = 0$ to $t = T_1$, as shown in Figure 2.2. The system of equations (2.3) has two families of characteristic lines with inclinations λ_1 and λ_2. When the Froude number ($\mathbf{Fr} = u/\sqrt{gh}$) is less than one, λ_1 is positive and λ_2 is negative; then only one condition is necessary on each boundary, since only one characteristic line reaches the boundary from inside the computational area. The condition is set only for the invariant corresponding to the outgoing characteristic, be-

cause the other invariant value is carried to the boundary along the incoming characteristic line. For example, the boundary condition for a totally reflective boundary $x = X_1$ is set for the Riemann invariant p as follows,

$$p = -q \tag{2.4}$$

while the reflective condition for the boundary $x = X_2$ is set for q, as

$$q = -p. \tag{2.5}$$

The existing finite-difference solutions of Hibberd and Peregrine (1979), Packwood (1980) and Kobayashi, et al. (1987) and their derivatives, all use the characteristic form of the equations to develop the seaward boundary conditions, however, they use the original form of the equations (2.1) for discretization. Since these solutions are not in terms of the characteristic variables, it is necessary to calculate one additional difference equation numerically, thereby introducing additional numerical error. Discretizing the characteristic form (2.3) directly makes possible the use of the exact expressions for Riemann invariants.

Gustafsson and Kreiss (1979) applied the characteristic approach to develop an absorbing boundary conditions for "arbitrary" time dependent problems. A totally absorbing boundary allows waves to go through (absorb) but it does not allow any waves to reflect back in the computation region. In characteristic terms, the invariant on outgoing characteristics does not carry any disturbances back into the computational area. Since only one boundary condition is necessary for the boundary $x = X_2$, the requirement of no wave motion on that characteristic implies that $u = 0$, $\eta = 0$, then $q = -2\sqrt{gd(x)}$. In addition, we assume that the water depth is constant outside the area of computation and equal to the

depth at the right boundary $d(X_2)$, then equation (2.3) implies that q is constant outside the area and on that boundary. Therefore, the appropriate condition is

$$q = -2\sqrt{gd(X_2)} \tag{2.6}$$

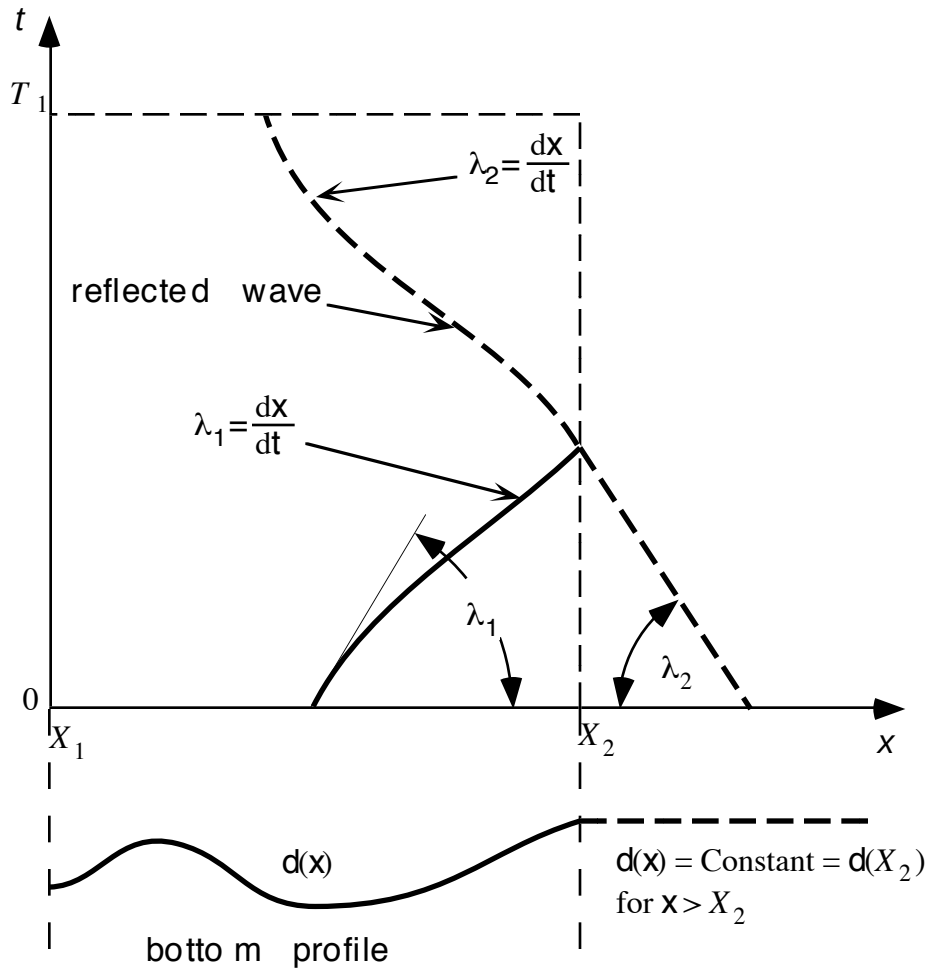

Figure 2.3 Sketch of the characteristic lines for the absorbing boundary condition.

Unfortunately, it is difficult to use the same approach for developing boundary conditions for the shoreline boundary for runup computations. The shoreline is moving, the

shoreline path is a characteristic line itself, and both incoming and outgoing characteristics cross and become one at the instantaneous shoreline point. This boundary condition is discussed in the next section.

2.3 The finite-difference method

2.3.1 The finite-difference scheme

A finite-difference form of (2.3) was developed using the method of undetermined coefficients assuming an explicit scheme and a second-order approximation of equations (2.3) in space and first-order in time. The method is described by Godunov (1971, section 7.22.2). It should be noted that no ad-hoc coefficients, no additional artificial-viscosity type or stabilizing algorithms are used. The proposed finite-difference form of equations (2.3) is:

$$\begin{aligned}&\frac{\Delta_t p_i^n}{\Delta t} + \frac{1}{2\Delta x}\left[\lambda_i^n\left(\Delta_{-x} + \Delta_x\right)p_i^n - \frac{\Delta t}{\Delta x}\lambda_i^n\Delta_x\left(\lambda_i^n\Delta_{-x}p_i^n\right)\right] = \\ &\frac{g}{2\Delta x}\left[\left(\Delta_{-x} + \Delta_x\right)d_i^n - \frac{\Delta t}{\Delta x}\lambda_i^n\Delta_x\Delta_{-x}d_i^n\right]\end{aligned} \tag{2.7}$$

where $f_i^n = f(x_i, t_n)$, Δx is space step, Δt is time increment, and

$$\begin{aligned}\Delta_t f_i^n &= f(x_i, t_n + \Delta t) - f(x_i, t_n) \\ \Delta_x f_i^n &= f(x_i + \Delta x, t_n) - f(x_i, t_n) \\ \Delta_{-x} f_i^n &= f(x_i, t_n) - f(x_i - \Delta x, t_n)\end{aligned} \tag{2.8}$$

The condition of the stability for the scheme is simply the Courant-Friedrichs-Lewy (CFL) criterion

$$\Delta t \le \frac{\Delta x}{|u| + \sqrt{gh}}. \tag{2.9}$$

implying that the wave should not propagate more than one grid point during the time step Δt.

The finite-difference equation (2.7) is used for the computation of the unknown variables p and q in the interior grid points of the computational area, but can not be used to compute boundary values. At those points, the boundary conditions (2.4) - (2.6) determine only one of the two invariants. The other value on the boundary (the value of the Riemann invariant on the incoming characteristic) is computed using one of the equations (2.3) approximated by an upwind scheme.

Good accuracy of numerical solutions of any hyperbolic equation is obtained whenever there are "enough" grid points per wave length. How many points are "enough" depends on the specific numerical method. The Lax-Wendroff method requires at least twenty grid points in one wave length to avoid the decay of the modeled waveform (Shuto et al, 1985). The proposed method only requires about ten points per wavelengths, as will be discussed later.

A variable grid method is used for consistent resolution throughout the flow domain. During shoaling, the wavelength becomes shorter. If one used a uniform grid throughout the computational domain then one would experience either loss of accuracy in the near-shore field or loss of efficiency through the use of very fine grid. Either approach does not produce consistent resolution. To allow for a variable grid with space step $\Delta x_i = x_{i+1} - x_i$, equations (2.7) are modified by replacing the first-order derivative operator

$$\frac{\left(\Delta_{-x} + \Delta_x\right)}{2\Delta x}, \tag{2.10}$$

by

$$\frac{\left(\Delta_{-x} + \Delta_x\right)}{\Delta x_{i-1} + \Delta x_i}, \tag{2.11}$$

The second-order derivative operator

$$\frac{\Delta_{-x}\Delta_x}{(\Delta x)^2} \tag{2.12}$$

is replaced by

$$\frac{2}{\Delta x_{i-1} + \Delta x_i}\Delta_x\left(\frac{\Delta_{-x}}{\Delta x_i}\right). \tag{2.13}$$

Operators above are described in equation (2.8). It is important to use the second order derivative operator in the form (2.13) instead of

$$\frac{4\Delta_{-x}\Delta_x}{\left(\Delta x_{i-1} + \Delta x_i\right)^2}. \tag{2.14}$$

The latter operator introduces a substantial zero-order truncation error associated with the grid ratio $s = \Delta x_i / \Delta x_{i+1}$; hence is not only inaccurate but also inconsistent.

Both operators (2.11) and (2.13) are correct to first order only, in comparison with the operator (2.12) appropriate for a uniform grid and correct to second order, because of the additional truncation error associated with the grid ratio *s*. Using more complicated operators with weighted values for the nonuniform grid scheme, it is possible to maintain sec-

ond-order accuracy in the first but not in the second derivative operators. However, the truncation error of (2.13) is the smallest possible among the 3-point second derivative approximations (Fletcher, C. A. J., 1991, section 10.1.5). For computational efficiency and for consistency in the order of approximation, (2.11) and (2.13) were used instead of using a higher order approximation for the first derivative.

The stability criterion (2.9) for this variable grid scheme becomes

$$\Delta t \le \min_i \frac{\Delta x_i}{|u_i| + \sqrt{g h_i}}. \tag{2.15}$$

To maintain the number of grid points per wave length constant during the wave propagation, the grid spacing must change with the wave celerity. Using the long wave approximation of the celerity

$$c = \sqrt{g d(x)}\,, \tag{2.16}$$

the grid ratio s is always given by

$$s = \frac{\Delta x_i}{\Delta x_{i+1}} = \frac{\sqrt{g d_i}}{\sqrt{g d_{i+1}}}. \tag{2.17}$$

Therefore, the Courant number remains nearly constant over the region where nonlinear effects are small. With this method, “linear” waves propagate exactly one space step during time period Δt, and the number of grid points per wave length remains constant.

On the dry bed, where $d(x) < 0$ c cannot be estimated a priori. In this region, a constant Δx equal to the smallest step in the "wet" area is used, assuming that the wave does not propagate faster on a dry land than over water. (See Synolakis (1986), figure 3.5.5, or Synolakis (1987b), figure 3.) For breaking waves, the bore propagation speed on dry land can be larger than the speed over water (Yeh et al, 1989, figure 6, and our Figure 2.15.) In this case the entire computation is reinstated with a smaller time step, until the CFL condition (2.15) is satisfied for the entire runup process.

2.3.2 The boundary conditions

To calculate the evolution on the dry bed, it is necessary to use moving boundary conditions. Here, the Froude number may be greater than one near the shoreline point, implying that both characteristic families have the same inclination in this region. Hence, it is impossible to use the direct relationships between the Riemann invariants of the type (2.4) - (2.6) near the shoreline. Therefore, approximations of the boundary values from previous space nodes are used as described in Figure 2.4.

The shoreline algorithm uses a time-dependent space step $\Delta x(t)$ of the last node of the computational area. The objective is maintain the shoreline boundary point (represented consecutively by A, B or C on Figure 2.4) on the surface of the beach during the computation. We therefore adjust the length of the last space step $\Delta x(t)$ every time step, so that the shoreline point (A) is at the intersection of the beach with the horizontal projection of the last "wet" point, for example n-1 node on Figure 2.4. The value of the velocity on the shoreline node is equal to the velocity on the previous "wet" point.

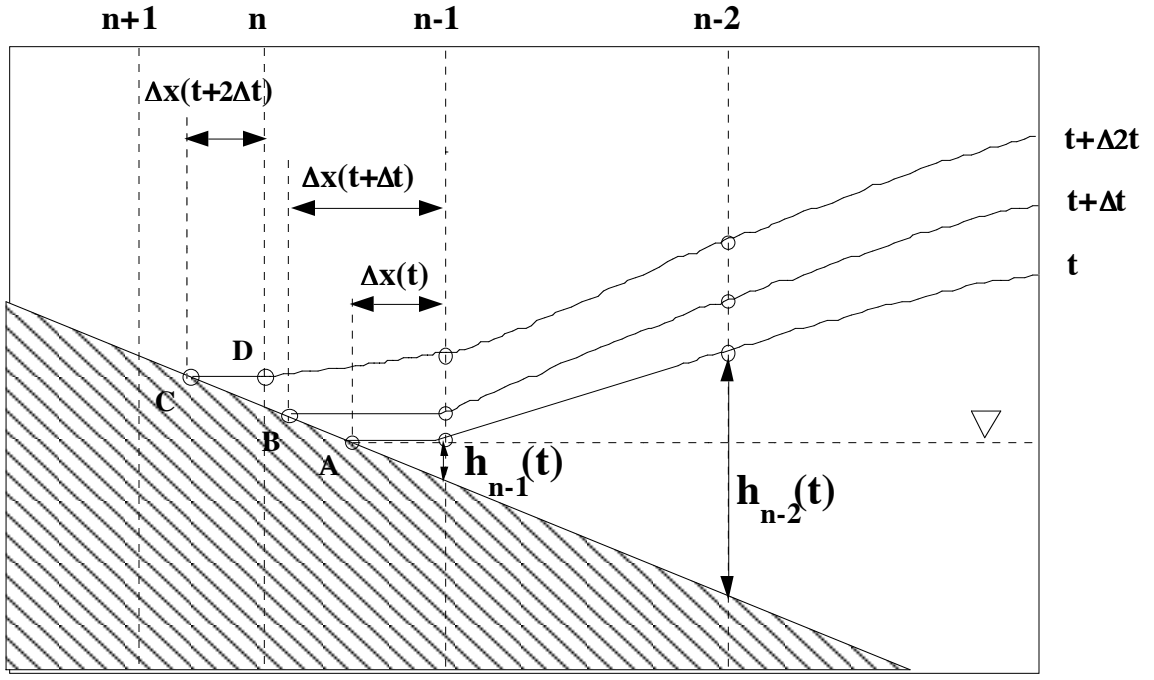

Figure 2.4 Definition sketch for shoreline computation

Additional grid points are introduced as follows. Referring to Figure 2.4, at the time interval between times t and $t + \Delta t$, there are n grid points (n-1 fixed grid points and the instantaneous shoreline, points A or B) in the computation. At time $t + 2\Delta t$, when the shoreline point (C) reaches beyond the next fixed grid point (n-th fixed node of the constant dry bed grid), this n-th fixed point is introduced between the shoreline point (C) and the previous internal fixed node (n-1) and $\eta(D) = \eta(C)$. Now, there are n+1 grid points in the computational area and we repeat the process. During rundown, we reduce the number of dry grid points sequentially in an analogous manner.

An absorbing boundary condition is used at the seaward boundary. As discussed earlier, q can be computed directly from (2.6). The other invariant p must be determined by the governing equations (2.3). The following simple first-order upwind scheme is then used to compute p

$$p_b^{n+1} = p_b^n - \frac{\Delta t}{\Delta x}\left[\lambda_1^n\left(\Delta_{-x} p_b^n\right) - g\left(\Delta_{-x} d_b^n\right)\right], \tag{2.18}$$

where p_b, d_b are values of the variables on the seaward boundary.

2.3.3 On dispersion, absorption and mass conservation

A series of simple numerical experiments was conducted to test the implementation of the absorbing boundary condition and to determine the minimum number of grid points per wavelength required to achieve propagation of "linear" waves with no change in shape. The experiments modeled the propagation of a long wave over a constant depth region. The left boundary of the computational area $x/d = 0$ was set to be reflective and described by the conditions (2.4), while the right boundary $x/d = 400$ was absorbing and is described by (2.6). The initial conditions were half-elliptical surface profile at the center of the computational area with a dimensionless amplitude $H/d = 0.01$ at the crest of the ellipse with zero initial velocity. This profile instead of a solitary wave profile was chosen, not only because it is steeper and thus a more serious test of the method than an equivalent solitary wave, but because it also allowed a definite number of grid points per wavelength; the effective wavelength of a solitary wave can be defined in various ways, but it is not always possible to ensure consistently an integer number of grid points per wavelength.

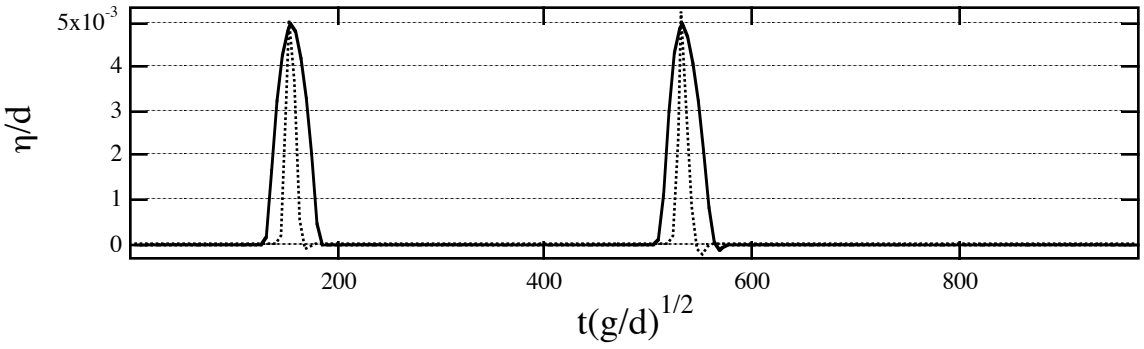

Figure 2.5 The results of numerical computation for checking the characteristics of VTCS-2 with a 0.005 elliptic wave propagating over constant depth region. Normalized surface elevations for two initial conditions (solid line *l/d = 50* and dotted line *l/d = 20*) as functions of the normalized time at 300 depths from the reflective boundary. The profiles on the left are the manifestations of the waves propagating towards the absorbing boundary, and the profiles near the center are the manifestations of the equivalent waves after reflecting off the reflective boundary as they propagate towards the absorbing boundary.

The initial profile produced two waves of the same shape with half of the initial amplitude propagating in opposite directions. The evenly-spaced numerical grid covered a computational area of 400 depths with 81 nodes, and the dimensionless time step was determined from (2.15) as $\Delta t\sqrt{g/d} = 4.85$. Different wavelengths were used for the computations. Typical results for semi-elliptic initial disturbances with dimensionless wavelengths *l/d* = 50 (solid line) and *l/d* = 20 (dotted line) corresponding to 10 and to 4 grid points per wavelength are shown on Figure 2.5, at 300 depths from the reflective boundary. Each of the two profiles on the left of the figure shows the wave coming from the source and propagating towards the absorbing boundary. Each profile near the center of the figure

is generated after reflection at the reflective boundary. On the other side the latter profiles do not show significant amplitude decay even for the shortest wave (represented only by 4 grid points), a wave which has already propagated 500 depths or 25 wavelengths. However effects of numerical dispersion are evident in the short wave which is modeled only with 4 grid points. There is no evidence of reflection from the absorbing boundary.

The mass conservation properties of the scheme were examined by monitoring the wave volume during test computations. Mass conservation requires that the total volume of the water involved in the computation remains constant (including the mass flax through the seaward boundary)

$$\int_{\Omega} h(x,t_0)dx = \int_{t_0}^{T} h\left(x_b,t\right)u\left(x_b,t\right)dt + \int_{\Omega} h(x,T)dx = Const \tag{2.19}$$

where Ω is the area of computation and x_b is the seaward boundary.

The mass conservation error $\varepsilon = (V_0 - V_t)/V_0$ remains within 0.01% during the computation of the semi-elliptic waves above, even for 4 grid points per wave length. The error is in the same range during the computation of the runup of solitary waves up a sloping beach, implying that, the moving boundary algorithm does not introduce substantial error into the computation.

Deviation from mass conservation are of concern during the breaking process and in subsequent evolution. The shallow-water wave theory is not valid anywhere near break-

ing and it does not allow for multivalued solutions. Yet, sufficient evidence suggesting that numerical results can be physically realistic exists to warrant numerical experimentation. However either mass conservation errors or "aliasing" errors can be expected. Aliasing errors emerge when the energy associated with shorter wavelengths reappears associated with longer wavelengths (Hamming, 1973). Mass conservation errors can emerge from the breakdown of the shallow-water wave model. Our computations of breaking-wave runup described in section 2.4 suggest that these errors increase with the initial wave height. For the highest modeled wave ($H/d = 0.3$), the mass conservation error was 0.7% between the beginning and the end of the computation, beyond rundown. This wave broke twice during the computation, both during runup and rundown, as did its laboratory manifestation.

The question arises whether this error is acceptable; only comparisons with the laboratory data can address this question. The comparisons with both laboratory and numerical data in section 2.4 suggest that this error does not quantitatively affect the predictions. One can argue that the differences observed in the details of some surface time histories are due to differences in dissipation rates and not in the mass conservation error. Also, Grilli (personal communication) solved a similar problem using potential theory and he reported an error of 1%, which occurred near breaking or shortly thereafter. The 1% error was his criterion for stopping the computation. The 0.7% error of this computation is clearly in the same range.